DALTON

The novel structure of the $[Au_{11}(PMePh_2)_{10}]^{3+}$ cation: crystal structures of $[Au_{11}(PMePh_2)_{10}][C_2B_9H_{12}]_3$·4thf and $[Au_{11}(PMePh_2)_{10}][C_2B_9H_{12}]_3$ (thf = tetrahydrofuran)

Royston C. B. Copley [a] **and D. Michael P. Mingos** *[,b]

[a] *Inorganic Chemistry Laboratory, University of Oxford, South Parks Road, Oxford OX1 3QR, UK*
[b] *Department of Chemistry, Imperial College of Science, Technology and Medicine, South Kensington, London SW7 2AY, UK*

Crystal structure analyses of $[Au_{11}(PMePh_2)_{10}][C_2B_9H_{12}]_3$·4thf (thf = tetrahydrofuran) and $[Au_{11}(PMePh_2)_{10}][C_2B_9H_{12}]_3$ showed the metal framework of the $[Au_{11}(PMePh_2)_{10}]^{3+}$ cation to approximate to a centred bicapped square antiprism, with idealized D_{4d} symmetry. Symmetry-related cage distances and angles have similar mean values but different ranges in the two structures, with the latter having greater consistency in the peripheral bond lengths but more distortion in the squares of the antiprism. It is suggested that these differences are directly related to the ligand packing around the metal skeletons. The cations of the two clusters cannot be superimposed in any orientation. It is possible to relate a centred bicapped square antiprism to the previously reported undecagold cage geometry, although they belong to different symmetry point groups. The largest differences between the idealized C_{3v} and D_{4d} frameworks centre around three adjacent peripheral sites. The movements required to interconvert the geometries take place about a common mirror plane and appear to be closely related to those of the diamond–square–diamond rearrangement mechanism. Fluxional interconversions of this type provide a possible explanation for the ^{31}P-$\{^1H\}$ NMR spectra of the Au_{11} cluster compounds.

The number of structurally characterized gold cluster compounds has risen steadily since the first investigation reported by McPartlin *et al.*[1] in 1969. In that study the metal framework found in $[Au_{11}(SCN)_3(PPh_3)_7]$ was described in terms of a pentagonal bipyramid and a square pyramid sharing a vertex. This portrayal is consistent with structural work[2–6] carried out on the compounds $[Au_{11}I_3\{P(C_6H_4F\text{-}p)_3\}_7]$, $[Au_{11}I_3(PPh_3)_7]$, $[Au_{11}(dppp)_5][SCN]_3$ [dppp = $Ph_2P(CH_2)_3PPh_2$], $[Au_{11}I(CNPr^i)_2(PPh_3)_7]$ and $[Au_{11}Cl_2(PPh_3)_8][OH]$ but later descriptions have emphasized the presence of a three-fold axis within the cage. The first of these descriptions views the structure down the three-fold axis of a centred chair, on one side of which is a basal triangle and on the other an apical atom. The second relates the cage to a centred icosahedral fragment in which one triangular face is replaced at its centre by a single atom. Either way, the geometries thus far reported can all be related to one basic C_{3v} template with minor distortions, probably resulting from ligand–ligand non-bonded interactions.

The cations $[Au_{11}(PMe_2Ph)_{10}]^{3+}$ and $[Au_{11}(PMePh_2)_{10}]^{3+}$ were first reported in 1981 and were prepared by the reduction of gold monomers using $[Ti(\eta\text{-}C_6H_5Me)_2]$.[7–9] Attempts to crystallize compounds containing these cations at the time proved unsuccessful but some reaction chemistry was investigated.[7,8] The addition of halides or pseudo-halides generally led to the formation of the centred icosahedral Au_{13} cluster compounds, typified by $[Au_{13}Cl_2(PMe_2Ph)_{10}][PF_6]_3$ which was structurally characterized.[9] Recently the $[Au_{11}(PMePh_2)_{10}]^{3+}$ cation has been used as a starting material for synthesizing mixed-metal icosahedral cluster compounds.[10]

^{31}P-$\{^1H\}$ NMR solution spectroscopy proves an extremely useful tool for monitoring and identifying the products of reactions involving gold cluster compounds. However, at room temperature, many of the spectra are singlets and do not show the range of environments expected on the basis of the solid-state structures. This is the case for compounds containing the $[Au_{11}(PMePh_2)_{10}]^{3+}$ cation. Clearly a process is averaging the different ^{31}P environments. The NMR studies on gold cluster compounds suggest that intermolecular exchange of gold–phosphine or phosphine groups is slow on the NMR time-scale.[11] A low-energy intramolecular process involving cage rearrangements is therefore the most probable explanation. The two skeletal isomers of the compound $[Au_9\{P(C_6H_4O\text{-}Me\text{-}p)_3\}_8][NO_3]_3$ provide some circumstantial evidence for this proposal.[12] Crystals of both isomers can be grown simultaneously and can be separated on the basis of their colour but in solution the ^{31}P-$\{^1H\}$ NMR spectra are identical. Further evidence for the occurrence of intramolecular skeletal rearrangements in gold clusters is presented in this paper.

Results and Discussion

The compound $[Au_{11}(PMePh_2)_{10}]^{3+}$ was synthesized by an adaptation of the method reported previously for $[Au_{11}(PMePh_2)_{10}][BPh_4]_3$ from $[AuCl(PMePh_2)]$ and di(toluene)titanium. The introduction of the unusual *nido*-carborane anion $C_2B_9H_{12}^-$ led to the isolation of suitable crystals for single-crystal X-ray analysis. Details of the characterization of the resulting compound $[Au_{11}(PMePh_2)_{10}][C_2B_9H_{12}]_3$ **1** are given in the Experimental section. The carborane salt **1** was prepared and crystallized in two different crystal modifications and single-crystal analyses were completed on both.

Crystal structure of cluster 1·4thf

Each asymmetric unit in cluster **1**·4thf (thf = tetrahydrofuran) contained an $[Au_{11}(PMePh_2)_{10}]^{3+}$ cation, three $[C_2B_9H_{12}]^-$ anions and five sites for thf molecules. The sum of the solvent occupancies was in the region of 3.8. This was rounded to the nearest integer for the purposes of defining the chemical formula and constants related to this. The inner co-ordination sphere of the $[Au_{11}(PMePh_2)_{10}]^{3+}$ cation found in **1**·4thf is shown in Fig. 1. Fig. 2 illustrates the numbering scheme

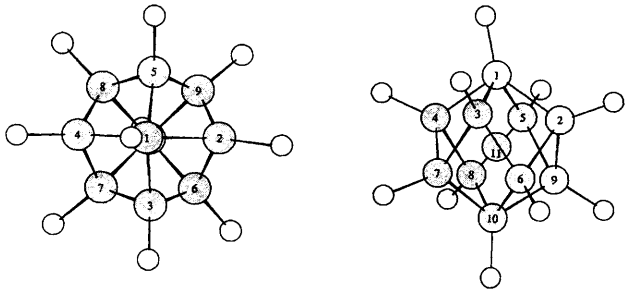

Fig. 1 The inner co-ordination sphere of the $[Au_{11}(PMePh_2)_{10}]^{3+}$ cation of cluster **1**·4thf. Phosphine substituents and bonds to the central atom are omitted for clarity. The visible metal framework is labelled with serial numbers for the gold atoms

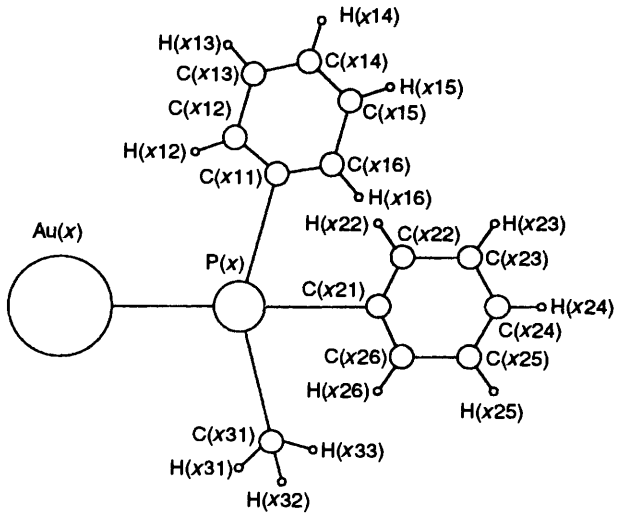

Fig. 2 The numbering scheme adopted for the phosphine ligands in cluster **1**·4thf

employed for the remaining atoms of the cation. A numbering scheme based on that previously used[13] was adopted for the anions. The first of the atoms in each anion are named B(101), B(201) and B(301); hydrogens were given the same serial number as the atom they were attached to; *endo*-hydrogens were not modelled. The atoms of the thf groups are numbered sequentially, starting from O(1), O(21), O(41), O(61) and O(81). Fractional atomic coordinates are listed in Table 1, whilst Tables 2 and 3, respectively, contain selected interatomic distances and a summary of selected interatomic angles for the cation. The metal cage is best described as a centred bicapped square antiprism (*CBSAPR*) and represents a departure from the geometry previously reported for undecagold cluster compounds. The total number of metal–metal bonds in the cation of **1**·4thf is lower than that reported for compounds with the idealized C_{3v} geometry and presumably results from the steric requirements of the bulky ligands. In the light of the cage geometry observed, the reactivity of the $[Au_{11}(PMePh_2)_{10}]^{3+}$ cation with $[M^{IB}Cl(PMePh_2)]$ (M^{IB} = Au, Ag or Cu), to give centred icosahedral cages, can be more easily understood:[10] such a reaction gives a cage that contains two more radial and eighteen additional tangential metal–metal bonds.

The information in Tables 2 and 3 is grouped assuming the idealized D_{4d} symmetry of the *CBSAPR*. The peripheral cage bonding distances can be divided into two categories. The average length of the bonds between the capping atoms and the square antiprism (distance category A, mean 2.907 ± 0.054 Å)* is somewhat shorter than the bonds between the squares of the antiprism (category B, mean 2.944 ± 0.048 Å). The significance of this difference is limited by the large range of lengths displayed within each group. The other distances of interest on the surface of the cage are those between the atoms forming the square faces of the antiprism (category C, mean 3.430 ± 0.143 Å). These interactions are regarded as non-bonding and as such the cage geometry may also be described as a centred bicapped crown.

As is generally the case for centred gold clusters, the radial metal–metal bonds are shorter and show less variation than their peripheral counterparts. The idealized D_{4d} symmetry divides the radial bonds into two categories. Those from the centre to the square antiprism (category D, mean 2.681 ± 0.016 Å) are shorter than those to the capping atoms (category E, mean 2.740 ± 0.012 Å). Unlike the peripheral bonds, the range of distances within each group is small, making the difference in average length more significant.

For a *CBSAPR* geometry the angles within the square faces of the antiprism should be 90°, whilst an angle of 180° is expected at the centre between the capping atoms. The values observed for the former in cluster **1**·4thf range between 86.05(3) and 92.91(3)°, with a mean of 89.96 ± 2.06°. The angle along the pseudo-four-fold axis is 175.76(4)°.

The bicapped square-antiprismatic geometry of the cage in the cation of cluster **1**·4thf is quite different from that reported[14] for $B_{10}H_{10}^{2-}$ because of the important radial metal–metal interactions. In $B_{10}H_{10}^{2-}$ the approximately equal boron–boron bond lengths lead to a prolate structure with the apical atoms significantly farther from the centroid than the atoms that define the square antiprism. In the $[Au_{11}(PMePh_2)_{10}]^{3+}$ cation of **1**·4thf the distance between the interstitial atom and the peripheral atoms is equalized at the expense of the bonds forming the square faces of the antiprism and the skeletal shape is more spherical. The structure is a bicapped adaptation of that reported for the orthorhombic modification of the $[Au_9\{P(C_6H_4OMe\text{-}p)_3\}_8]^{3+}$ cluster cation.[12,15] Comparable distances for $[Au_9\{P(C_6H_4OMe\text{-}p)_3\}_8][BF_4]_3$ are presented in Table 4. The largest difference is seen in the mean length of the peripheral bonds within the crown, distance category B. As a result the distance between the two squares of the antiprism is reduced from 2.28 Å in **1**·4thf to 2.11 Å. Such a contraction is energetically favourable if the steric requirements of the ligands can be met. In the absence of phosphine groups along the four-fold axis, the bulky ligands in the nonagold cluster move away from one another and towards the open areas on either side of the crown. This is clearly reflected in the angle subtended at the peripheral cage positions between the bonded phosphorus atoms and the central gold. In $[Au_9\{P(C_6H_4OMe\text{-}p)_3\}_8][BF_4]_3$ these angles range between 161.4(4) and 165.3(4)°, as compared to between 171.2(2) and 178.4(2)° in **1**·4thf.

Another cluster compound that can be related to **1**·4thf is $[Pt(AuPPh_3)_8Hg_2][NO_3]_4$. The cation also displays a geometry based on that of a *CBSAPR* and has a central platinum, with two mercury atoms capping a gold crown.[16] Mean distances within the cages of $[Pt(AuPPh_3)_8Hg_2][NO_3]_4$ and **1**·4thf are given in Table 4. The crown arrangements in the two cations contain similar peripheral bonding distances and a separation of 2.28 Å between the squares of each antiprism. The presence of a platinum atom in the heteronuclear case has the effect of shortening the radial distances to the crown and this is reflected in somewhat shorter contacts within the square faces of the antiprism. The long Pt–Hg radial distances lead to an elongation of the *CBSAPR* along the four-fold axis when compared to **1**·4thf. As discussed for $[Au_9\{P(C_6H_4OMe\text{-}p)_3\}_8][BF_4]_3$, the absence of ligands along the principal cage axis in $[Pt(AuPPh_3)_8Hg_2][NO_3]_4$ allows the phosphine groups to move further away from one another. At a peripheral cage

* The sample standard deviation is provided after all mean values in this paper and is defined as: $\sigma_{n-1} = [\{\Sigma x^2 - [(\Sigma x)^2/n]\}/(n-1)]^{\frac{1}{2}}$ where: σ_{n-1} = sample standard deviation, Σx^2 = sum of the squared observations, $(\Sigma x)^2$ = sum of the observations squared and n = number of observations.

Table 1 Fractional atomic coordinates for cluster **1**·4thf

Atom	*x*	*y*	*z*	Atom	*x*	*y*	*z*
Au(1)	0.757 81(4)	0.582 96(3)	0.271 47(4)	C(721)	0.536 5(8)	0.481 7(6)	0.155(1)
Au(2)	0.798 04(4)	0.510 15(3)	0.352 76(3)	C(722)	0.532 4(8)	0.494 6(8)	0.101 3(9)
Au(3)	0.668 42(4)	0.527 38(3)	0.306 70(4)	C(723)	0.501 8(9)	0.534 3(8)	0.085 8(7)
Au(4)	0.716 73(4)	0.535 75(3)	0.174 44(3)	C(724)	0.475 4(8)	0.561 2(6)	0.124(1)
Au(5)	0.845 17(3)	0.526 75(3)	0.232 75(4)	C(725)	0.479 6(8)	0.548 3(7)	0.177 6(9)
Au(6)	0.711 71(4)	0.432 90(3)	0.338 60(4)	C(726)	0.510 2(9)	0.508 6(8)	0.193 1(7)
Au(7)	0.656 65(4)	0.455 09(3)	0.221 63(4)	C(731)	0.591 0(9)	0.395 2(9)	0.123(1)
Au(8)	0.790 28(4)	0.455 59(3)	0.165 09(3)	C(811)	0.774 3(8)	0.390 1(7)	0.048 2(8)
Au(9)	0.842 68(3)	0.434 22(3)	0.284 97(3)	C(812)	0.726 5(9)	0.376 0(8)	0.071 5(6)
Au(10)	0.746 58(4)	0.388 93(3)	0.239 69(4)	C(813)	0.691 8(7)	0.344 4(8)	0.044 7(8)
Au(11)	0.752 55(3)	0.485 10(3)	0.259 53(3)	C(814)	0.704 9(8)	0.326 9(7)	−0.005 4(8)
P(1)	0.753 4(2)	0.665 4(2)	0.266 3(2)	C(815)	0.752 8(9)	0.341 1(8)	−0.028 7(6)
P(2)	0.827 5(3)	0.524 8(2)	0.439 4(2)	C(816)	0.787 5(8)	0.372 7(8)	−0.001 9(8)
P(3)	0.599 6(3)	0.569 8(2)	0.344 1(3)	C(821)	0.833(1)	0.479 2(7)	0.038 6(9)
P(4)	0.680 6(3)	0.579 0(2)	0.103 7(2)	C(822)	0.797 3(9)	0.493(1)	−0.002(1)
P(5)	0.920 7(2)	0.566 0(2)	0.206 5(2)	C(823)	0.809(1)	0.533(1)	−0.033 0(8)
P(6)	0.676 6(3)	0.381 9(2)	0.401 3(3)	C(824)	0.856(1)	0.559 4(7)	−0.023 0(9)
P(7)	0.578 3(3)	0.431 4(2)	0.179 2(3)	C(825)	0.891 5(9)	0.545(1)	0.018(1)
P(8)	0.820 0(3)	0.430 6(2)	0.083 9(2)	C(826)	0.880(1)	0.505(1)	0.048 6(8)
P(9)	0.913 8(2)	0.386 9(2)	0.312 1(2)	C(831)	0.884(1)	0.398 3(9)	0.088 2(9)
P(10)	0.751 5(3)	0.309 4(2)	0.216 3(3)	C(911)	0.980 6(4)	0.414 6(5)	0.319 8(6)
C(111)	0.814 3(5)	0.696 1(6)	0.246 4(7)	C(912)	0.984 9(5)	0.464 2(5)	0.316 7(6)
C(112)	0.859 0(7)	0.690 3(6)	0.280 7(5)	C(913)	1.035 1(6)	0.486 0(4)	0.323 6(7)
C(113)	0.908 0(6)	0.711 5(6)	0.268 7(7)	C(914)	1.080 9(4)	0.458 3(6)	0.333 7(7)
C(114)	0.912 3(5)	0.738 6(6)	0.222 3(7)	C(915)	1.076 6(5)	0.408 7(6)	0.336 9(7)
C(115)	0.867 7(7)	0.744 4(6)	0.188 0(6)	C(916)	1.026 4(6)	0.386 8(4)	0.330 0(7)
C(116)	0.818 7(6)	0.723 2(6)	0.200 1(6)	C(921)	0.926 6(6)	0.335 1(4)	0.269 4(5)
C(121)	0.732 6(9)	0.696 4(6)	0.325 4(6)	C(922)	0.938 5(7)	0.344 8(4)	0.216 5(5)
C(122)	0.722 4(9)	0.670 4(4)	0.371 4(8)	C(923)	0.950 5(7)	0.307 5(5)	0.181 9(4)
C(123)	0.704 9(9)	0.693 8(7)	0.416 9(6)	C(924)	0.950 4(7)	0.260 5(4)	0.200 2(5)
C(124)	0.697 7(9)	0.743 2(7)	0.416 3(7)	C(925)	0.938 4(7)	0.250 7(3)	0.253 1(5)
C(125)	0.707 9(9)	0.769 3(5)	0.370 2(8)	C(926)	0.926 5(7)	0.288 0(5)	0.287 7(4)
C(126)	0.725 4(9)	0.745 8(6)	0.324 8(6)	C(931)	0.902 5(8)	0.361 1(7)	0.377 1(8)
C(131)	0.701(1)	0.684 2(9)	0.218(1)	C(1011)	0.687 8(6)	0.282 0(6)	0.191 6(7)
C(211)	0.851 4(7)	0.584 6(4)	0.454 1(6)	C(1012)	0.686 6(6)	0.246 9(6)	0.152 2(7)
C(212)	0.877 8(7)	0.594 7(5)	0.502 5(6)	C(1013)	0.637 7(8)	0.226 3(5)	0.136 0(6)
C(213)	0.891 4(7)	0.641 7(5)	0.515 5(5)	C(1014)	0.590 0(6)	0.240 8(6)	0.159 2(7)
C(214)	0.878 4(7)	0.678 6(4)	0.480 0(7)	C(1015)	0.591 2(6)	0.276 0(6)	0.198 7(7)
C(215)	0.852 0(7)	0.668 5(4)	0.431 6(6)	C(1016)	0.640 1(7)	0.296 6(5)	0.214 9(6)
C(216)	0.838 5(7)	0.621 5(5)	0.418 6(5)	C(1021)	0.776 6(7)	0.270 6(5)	0.269 8(6)
C(221)	0.882 5(6)	0.487 5(5)	0.464 6(7)	C(1022)	0.781 9(7)	0.288 1(4)	0.321 7(7)
C(222)	0.877 8(6)	0.460 1(7)	0.510 6(7)	C(1023)	0.801 2(7)	0.258 5(6)	0.362 6(5)
C(223)	0.920 9(8)	0.432 0(6)	0.528 8(6)	C(1024)	0.815 4(7)	0.211 4(5)	0.351 6(6)
C(224)	0.968 7(7)	0.431 4(6)	0.500 9(8)	C(1025)	0.810 1(8)	0.193 8(4)	0.299 8(7)
C(225)	0.973 5(6)	0.458 8(7)	0.454 9(7)	C(1026)	0.790 8(8)	0.223 4(6)	0.258 8(5)
C(226)	0.930 3(7)	0.486 9(6)	0.436 7(6)	C(1031)	0.799 7(9)	0.297 3(8)	0.165(1)
C(231)	0.773(1)	0.513 2(8)	0.484 1(8)	B(101)	−0.051 9(5)	0.321 1(5)	−0.029 1(6)
C(311)	0.534 9(6)	0.540 5(7)	0.345 8(8)	B(102)	−0.009 2(6)	0.323 3(4)	0.028 3(5)
C(312)	0.533 6(6)	0.491 8(7)	0.357 5(8)	B(103)	0.017 7(6)	0.333 5(4)	−0.035 1(6)
C(313)	0.484 3(8)	0.468 1(5)	0.359 4(9)	B(104)	−0.015 2(6)	0.295 3(5)	−0.081 7(4)
C(314)	0.436 4(6)	0.493 0(7)	0.349 7(9)	B(105)	−0.061 1(5)	0.259 4(5)	−0.047 5(5)
C(315)	0.437 8(6)	0.541 7(7)	0.337 9(8)	B(106)	−0.057 0(5)	0.276 5(5)	0.022 5(5)
C(316)	0.487 0(8)	0.565 5(5)	0.336 0(8)	C(107)	0.048 4(4)	0.294 5(5)	0.008 7(5)
C(321)	0.583 6(7)	0.625 3(5)	0.311 5(6)	C(108)	0.044 0(5)	0.277 9(5)	−0.050 0(5)
C(322)	0.569 3(7)	0.622 5(4)	0.257 5(6)	B(109)	0.002 3(6)	0.235 1(4)	−0.062 9(5)
C(323)	0.553 0(7)	0.663 4(6)	0.229 8(5)	B(110)	−0.028 4(6)	0.221 7(4)	0.000 5(6)
C(324)	0.551 0(8)	0.707 3(5)	0.256 2(7)	B(111)	0.009 5(6)	0.262 9(5)	0.045 7(4)
C(325)	0.565 3(8)	0.710 1(4)	0.310 2(7)	B(201)	0.484(1)	0.766(1)	−0.021(1)
C(326)	0.581 6(7)	0.669 2(6)	0.337 9(5)	B(202)	0.451 2(9)	0.743(1)	0.035(1)
C(331)	0.613(1)	0.585(1)	0.413(1)	B(203)	0.510(1)	0.777 0(8)	0.045(1)
C(411)	0.724 1(7)	0.627 5(6)	0.079 3(9)	B(204)	0.554(1)	0.765(1)	−0.008(1)
C(412)	0.779 3(7)	0.619 9(6)	0.074 7(9)	B(205)	0.525(1)	0.720(1)	−0.0481(7)
C(413)	0.812 3(5)	0.656 9(7)	0.057 3(9)	B(206)	0.459(1)	0.706(1)	−0.021(1)
C(414)	0.790 0(8)	0.701 4(6)	0.044 7(9)	C(207)	0.505(1)	0.722(1)	0.073 4(7)
C(415)	0.734 8(8)	0.708 9(6)	0.049 4(9)	C(208)	0.561(1)	0.734(1)	0.051(1)
C(416)	0.701 8(6)	0.671 9(7)	0.066 7(9)	B(209)	0.575 4(9)	0.704(1)	−0.001(1)
C(421)	0.660 4(9)	0.543 8(8)	0.045 8(7)	B(210)	0.516(1)	0.666 7(8)	−0.011(1)
C(422)	0.668 9(9)	0.494 5(8)	0.046 2(7)	B(211)	0.469(1)	0.681(1)	0.044(1)
C(423)	0.653(1)	0.467 1(6)	0.002 0(9)	B(301)	0.694(1)	0.921 4(7)	0.123(1)
C(424)	0.629(1)	0.488 9(8)	−0.042 7(7)	B(302)	0.699(1)	0.893(1)	0.060 1(9)
C(425)	0.621(1)	0.538 2(9)	−0.043 1(7)	B(303)	0.643 3(9)	0.881(1)	0.100(1)
C(426)	0.636(1)	0.565 7(6)	0.001 1(9)	B(304)	0.667(1)	0.879(1)	0.167(1)
C(431)	0.620 3(9)	0.609 7(9)	0.119 8(9)	B(305)	0.737(1)	0.889(1)	0.169(1)
C(511)	0.962 3(6)	0.590 4(5)	0.262 4(6)	B(306)	0.758(1)	0.899(1)	0.101(1)
C(512)	0.940 4(5)	0.592 6(5)	0.312 9(7)	C(307)	0.679(1)	0.835 5(9)	0.073(1)
C(513)	0.970 0(7)	0.612 7(6)	0.355 2(5)	C(308)	0.661(1)	0.827 2(9)	0.130(1)

Table 1 (*Contd.*)

Atom	*x*	*y*	*z*	Atom	*x*	*y*	*z*
C(514)	1.021 5(6)	0.630 7(5)	0.347 1(6)	B(309)	0.714(1)	0.829(1)	0.168 6(9)
C(515)	1.043 4(4)	0.628 5(5)	0.296 6(7)	B(310)	0.775 9(9)	0.845(1)	0.136(1)
C(516)	1.013 9(6)	0.608 3(6)	0.254 2(5)	B(311)	0.744(1)	0.843(1)	0.068(1)
C(521)	0.968 4(7)	0.530 9(5)	0.168 7(7)	O(1)	0.374(2)	0.626(2)	0.222(1)
C(522)	0.972 2(7)	0.482 4(6)	0.180 9(6)	C(2)	0.334(2)	0.615(1)	0.182(2)
C(523)	1.004 5(7)	0.452 5(4)	0.150 7(8)	C(3)	0.339(2)	0.653(2)	0.138(1)
C(524)	1.033 1(7)	0.471 3(6)	0.108 4(7)	C(4)	0.359(2)	0.696(1)	0.169(2)
C(525)	1.029 3(7)	0.519 8(6)	0.096 3(6)	C(5)	0.396(2)	0.673(2)	0.212(2)
C(526)	0.996 9(8)	0.549 6(5)	0.126 4(7)	O(21)	0.716(1)	0.087(2)	0.129(2)
C(531)	0.905(1)	0.617 3(8)	0.165(1)	C(22)	0.759(3)	0.059(1)	0.108(2)
C(611)	0.624 8(7)	0.407 4(6)	0.444 0(7)	C(23)	0.811(2)	0.073(2)	0.139(2)
C(612)	0.638 0(6)	0.450 3(6)	0.469 5(8)	C(24)	0.800(2)	0.124(2)	0.153(2)
C(613)	0.601 8(8)	0.471 4(5)	0.503 9(7)	C(25)	0.739(2)	0.124(2)	0.162(2)
C(614)	0.552 3(7)	0.449 6(6)	0.512 8(7)	O(41)	0.103(2)	0.331(1)	0.140(2)
C(615)	0.539 1(6)	0.406 7(7)	0.487 3(8)	C(42)	0.158(2)	0.337(2)	0.123(2)
C(616)	0.575 3(8)	0.385 6(5)	0.452 9(7)	C(43)	0.191(1)	0.356(2)	0.170(3)
C(621)	0.723 3(7)	0.354 6(6)	0.449 5(6)	C(44)	0.149(3)	0.383(2)	0.201(2)
C(622)	0.777 8(8)	0.366 6(5)	0.448 6(6)	C(45)	0.098(2)	0.353(2)	0.191(2)
C(623)	0.814 8(6)	0.343 0(7)	0.482 1(7)	O(61)	0.170(2)	0.576(2)	0.146(2)
C(624)	0.797 3(7)	0.307 4(7)	0.516 5(7)	C(62)	0.130(2)	0.581(2)	0.186(3)
C(625)	0.742 8(8)	0.295 5(6)	0.517 4(7)	C(63)	0.143(3)	0.545(3)	0.229(2)
C(626)	0.705 8(6)	0.319 1(7)	0.483 9(8)	C(64)	0.170(3)	0.505(2)	0.199(3)
C(631)	0.643(1)	0.330 5(9)	0.369(1)	C(65)	0.200(2)	0.534(2)	0.157(2)
C(711)	0.531 1(8)	0.396 1(6)	0.218(1)	O(81)	0.370(2)	0.446(3)	0.200(2)
C(712)	0.542 2(7)	0.386 2(7)	0.272(1)	C(82)	0.334(4)	0.487(2)	0.199(3)
C(713)	0.507(1)	0.357 6(8)	0.300 1(8)	C(83)	0.279(2)	0.469(3)	0.180(3)
C(714)	0.461 0(9)	0.338 9(7)	0.275(1)	C(84)	0.294(3)	0.428(3)	0.144(3)
C(715)	0.449 9(7)	0.348 8(8)	0.221(1)	C(85)	0.343(3)	0.407(2)	0.173(3)
C(716)	0.485(1)	0.377 4(8)	0.192 8(8)				

position the mean angle between the bonded phosphorus atom and the central gold is 166.35 ± 0.09° in the mixed-metal cluster. In **1**·4thf the mean for the corresponding eight angles is 174.88 ± 2.16°.

Crystal structure of cluster 1

The asymmetric unit of cluster **1** contains an $[Au_{11}(PMePh_2)_{10}]^{3+}$ cation, two disordered $[C_2B_9H_{12}]^-$ groups and a region of residual electron density, assumed to be the site of the third anion. As in **1**·4thf, the metal framework of **1** has a *CBSAPR* geometry and idealized D_{4d} symmetry. Fractional atomic coordinates for **1** are given in Table 5. The numbering scheme for the cation is identical to that used for **1**·4thf. The two disordered anions are numbered sequentially from B(100) and B(200). Selected interatomic distances and a summary of selected interatomic angles are given in Tables 6 and 7, respectively, where the information is grouped as before. Comparing the bond lengths and angles for **1**·4thf and **1**, the mean values in the various categories are very similar: the difference in the means is never greater than either of the associated standard deviations. The ranges vary far more. Consider, for example, the peripheral cage distances. For bond-length categories A and B the range is three times smaller in **1**. For category C however the range is twice as large. This can be summarized by saying that in **1** there is greater consistency in the peripheral bond lengths but more distortion in the squares of the antiprism. The latter point means that the cation in **1** appears to resemble the *CBSAPR* a little less than that in **1**·4thf.

Ligand packing in clusters 1·4thf and 1

Fig. 3 illustrates the packing of the $PMePh_2$ groups around the metal frameworks in clusters **1**·4thf and **1**. The ligand arrangements are not identical in any orientation of the cations but many similarities may be identified, particularly when the cations are compared in the manner shown.

The orientation of each of the phosphines in clusters **1** was assessed by examining the direction of the P–C bonds and the position of the methyl group relative to the cage. Using these criteria the crown ligand arrangements were found to be similar and to be approximately related by the symmetry operators of the point group D_4. In each case a bond to one phenyl group is almost *trans* to a cage bond between a crown and a capping gold atom. Examples of this can be seen in Fig. 3(*b*) around Au(7) and Au(9). The same figure shows the largest departure from the exact *trans* relationship: at Au(6), the deviation is equivalent to a 29° rotation about the metal–ligand bond. Widening the discussion to include the orientations of the phenyl groups, the pseudo-symmetry described above is lost. The planar rings adopt positions that lower the interactions between neighbouring groups. The ligands attached to the capping gold atoms are essentially staggered relative to one another: projected along the pseudo-four-fold axis the angle between the two P–Me bonds is 51°.

Considering the phosphine-ligand packing in the cations of clusters **1** and **1**·4thf two major differences can be recognized. The first concerns the orientation of the phosphine group bonded to Au(2) in **1**·4thf. Compared to Au(6) in **1**, a rotation of 128° has occurred about the Au–P bond. Probably as a result of this, the second major difference is seen in the relative orientations of the apical phosphines. These are no longer staggered and the projected angle between the two P–Me bonds is 90°. The ligands bonded to Au(1) and Au(2) in **1**·4thf clearly bend apart. Distortions of this type and the rotations described above lead to the conclusion that the packing in **1**·4thf is less regular than that seen in **1**.

Having considered the ligand arrangements in clusters **1** and **1**·4thf, the ranges of the peripheral distances in Tables 2 and 6 can be rationalized. For the distances in categories A and B the spread of lengths is three times greater for the cation in **1**·4thf. This finding is in keeping with the description of the more disturbed ligand packing. In each category the distances to the rotated Au(2) are atypical. The distances in category C are dependent on the orientation of the apical ligands and, in particular, the positions of the phenyl groups: the range is greater for **1**, where all four of the phenyl groups are on one side of the cage.

Table 2 Selected interatomic distances (Å) for the cation of cluster **1**·4thf

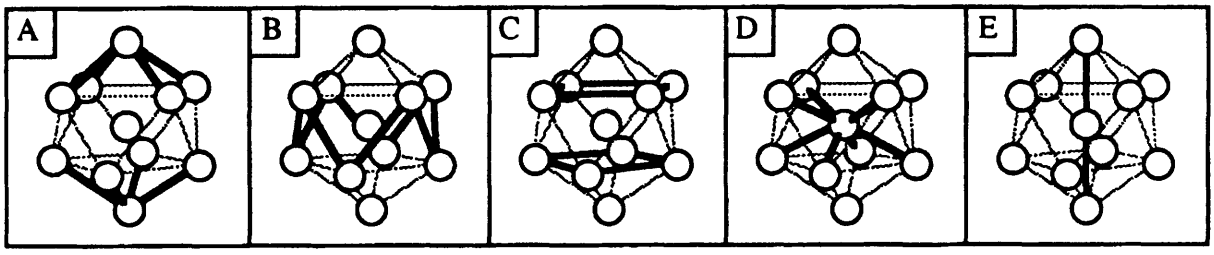

Peripheral cage		Radial cage	
Category A		Category D	
Au(1)–Au(2)	3.024(1)	Au(2)–Au(11)	2.656(1)
Au(1)–Au(3)	2.860(1)	Au(3)–Au(11)	2.692(1)
Au(1)–Au(4)	2.920(1)	Au(4)–Au(11)	2.685(1)
Au(1)–Au(5)	2.860(1)	Au(5)–Au(11)	2.671(1)
Au(6)–Au(10)	2.913(1)	Au(6)–Au(11)	2.676(1)
Au(7)–Au(10)	2.917(1)	Au(7)–Au(11)	2.667(1)
Au(8)–Au(10)	2.867(1)	Au(8)–Au(11)	2.693(1)
Au(9)–Au(10)	2.897(1)	Au(9)–Au(11)	2.705(1)
Range 2.860(1)–3.024(1), mean 2.907 ± 0.054		2.656(1)–2.705(1), 2.681 ± 0.016	
Category B		Category E	
Au(2)–Au(6)	3.048(1)	Au(1)–Au(11)	2.748(1)
Au(2)–Au(9)	2.946(1)	Au(10)–Au(11)	2.731(1)
Au(3)–Au(6)	2.946(1)	2.731(1)–2.748(1), 2.740 ± 0.012	
Au(3)–Au(7)	2.940(1)		
Au(4)–Au(7)	2.959(1)		
Au(4)–Au(8)	2.896(1)		
Au(5)–Au(8)	2.920(1)		
Au(5)–Au(9)	2.894(1)	Au(x)–P(x)	
Range 2.894(1)–3.048(1), mean 2.944 ± 0.048		Au(1)–P(1)	2.305(5)
		Au(2)–P(2)	2.305(6)
Category C		Au(3)–P(3)	2.293(6)
Au(2)–Au(3)	3.413(1)	Au(4)–P(4)	2.302(6)
Au(2)–Au(5)	3.283(1)	Au(5)–P(5)	2.278(6)
Au(3)–Au(4)	3.556(1)	Au(6)–P(6)	2.304(6)
Au(4)–Au(5)	3.471(1)	Au(7)–P(7)	2.284(7)
Au(6)–Au(7)	3.254(1)	Au(8)–P(8)	2.288(6)
Au(6)–Au(9)	3.541(1)	Au(9)–P(9)	2.288(5)
Au(7)–Au(8)	3.632(1)	Au(10)–P(10)	2.299(6)
Au(8)–Au(9)	3.290(1)	2.278(6)–2.305(6), 2.295 ± 0.010	
Range 3.254(1)–3.632(1), mean 3.430 ± 0.143			

Cage geometries adopted by undecagold cluster compounds

The cation $[Au_{11}(PMePh_2)_{10}]^{3+}$ found in clusters **1**·4thf and **1** has been shown to have a metal skeleton that possesses approximate four-fold symmetry. The previously reported undecagold cages have been similar to one another and have contained either a pseudo- or a crystallographically imposed three-fold axis. Conditioned by illustrations that emphasize these rotational symmetry operators, it is initially difficult to recognize any similarities between the two basic geometries. The metal frameworks found in **1**·4thf and $[Au_{11}Cl_2(PPh_3)_8][OH]$ **2** are representative of the Au_{11} cluster geometries and are illustrated in Fig. 4. Unless stated to the contrary, discussions referring to this figure use the numbering scheme of **1**·4thf to identify atom positions. In the orientations shown the two cages do not appear too dissimilar. The apical positions in the metal framework of **1**·4thf are related to two atoms opposite one another in the chair of **2**.

Whilst there are many subtle differences between the cages found in clusters **1**·4thf and **2**, the major ones seem to centre around the positions of atoms 2, 6 and 9. The essence of the relationship between the geometries can be described in terms of three cage deformations which all but convert the former framework into the latter. These are: (*i*) a rotation of 2 towards 10, (*ii*) a separation of 6 and 9 and (*iii*) a translation of 3 and 5 towards 4. The motions described take place about a mirror plane passing through positions 1, 2, 4, 10 and 11. As viewed in Fig. 4, this mirror represents the only symmetry element common to both geometries. The movements associated with steps (*i*) and (*ii*) above resemble those expected for a diamond–square–diamond (d.s.d.) rearrangement.[17] Such a mechanism has been used to explain rearrangements of the *CBSAPR* geometry[17] for compounds such as $B_{10}H_8(NMe_3)_2$. In converting between D_{4d} arrangements using the d.s.d. mechanism a C_{3v} intermediate can be recognized.[18] This appears very similar to the Au_{11} geometry that has been reported in the past.

^{31}P-$\{^1H\}$ Solution NMR studies

The solution ^{31}P-$\{^1H\}$ NMR spectrum of $[Au_{11}(PMePh_2)_{10}]^{3+}$ consists of a sharp singlet, even at low temperatures. This is not consistent with the solid-state structure. The

Table 3 Summary of selected interatomic angles (°) for the cation of cluster **1**·4thf

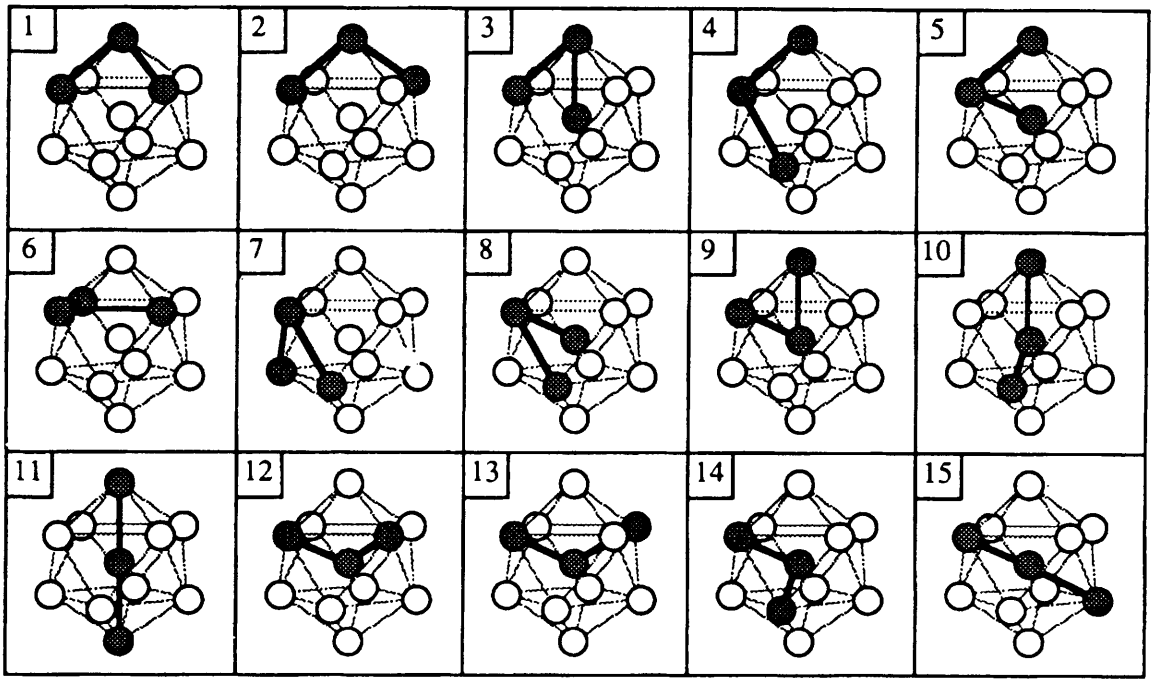

Cage angle category		
1	**2**	**3**
Range 67.77(3)–77.79(3)	110.94(3)–113.94(4)	54.55(3)–57.45(3)
Mean 72.34 ± 3.83	113.09 ± 1.44	56.59 ± 0.95
4	**5**	**6**
Range 98.81(4)–108.07(4)	57.43(3)–59.46(3)	86.05(3)–92.91(3)
Mean 102.90 ± 2.53	58.54 ± 0.63	89.96 ± 2.06
7	**8**	**9**
Range 67.12(3)–76.65(3)	54.83(3)–58.00(3)	63.41(3)–68.02(3)
Mean 71.29 ± 3.32	56.69 ± 0.83	64.87 ± 1.47
10	**11**	**12**
Range 110.93(4)–118.53(4)	175.76(4)	75.05(4)–85.31(4)
Mean 115.17 ± 2.81		79.59 ± 3.87
13	**14**	**15**
Range 126.76(4)–132.92(4)	65.13(3)–69.72(3)	134.60(4)–143.99(4)
Mean 129.60 ± 2.55	66.61 ± 1.45	139.41 ± 3.43
Au(11)–Au(*x*)–P(*x*)		
Range 169.2(2)–178.4(2), mean 174.06 ± 2.67		

Table 4 Mean cage distances (Å) in two cluster compounds where the metal frameworks are geometrically related to that found for **1**·4thf

	Cage distance category				
Cluster	A	B	C	D	E
1·4thf	2.907 ± 0.054	2.944 ± 0.048	3.430 ± 0.143	2.681 ± 0.016	2.740 ± 0.012
$[Au_9\{P(C_6H_4OMe\text{-}p)_3\}_8][BF_4]_3$	—	2.818 ± 0.015	3.461 ± 0.056	2.664 ± 0.010	—
$[Pt(AuPPh_3)_8Hg_2][NO_3]_4$	3.004 ± 0.003	2.917 ± 0.014	3.353 ± 0.029	2.632 ± 0.001	2.987 ± 0.063

Table 5 Fractional atomic coordinates for cluster **1**

Atom	*x*	*y*	*z*	Atom	*x*	*y*	*z*
Au(1)	0.141 62(4)	−0.133 94(4)	0.689 93(2)	C(613)	0.425(1)	−0.205(1)	0.907 8(5)
Au(2)	0.242 70(4)	−0.180 77(4)	0.759 08(2)	C(614)	0.433(1)	−0.221(1)	0.952 8(5)
Au(3)	0.149 78(4)	−0.025 72(5)	0.774 13(2)	C(615)	0.400(1)	−0.184(1)	0.984 3(4)
Au(4)	0.213 03(4)	0.056 82(4)	0.685 74(2)	C(616)	0.361(1)	−0.132(1)	0.970 8(4)
Au(5)	0.302 78(4)	−0.072 94(4)	0.659 79(2)	C(621)	0.212 2(7)	−0.071 2(9)	0.933 3(4)
Au(6)	0.295 46(4)	−0.027 98(5)	0.833 11(2)	C(622)	0.166 7(9)	−0.156 4(8)	0.941 5(5)
Au(7)	0.300 78(4)	0.141 25(4)	0.782 18(2)	C(623)	0.093 6(9)	−0.176 9(8)	0.959 2(5)
Au(8)	0.398 46(4)	0.113 36(4)	0.705 69(2)	C(624)	0.065 9(7)	−0.112(1)	0.968 8(5)
Au(9)	0.413 56(4)	−0.065 95(4)	0.745 71(2)	C(625)	0.111(1)	−0.027(1)	0.960 6(5)
Au(10)	0.443 73(4)	0.097 38(4)	0.802 10(2)	C(626)	0.184 5(9)	−0.006 5(7)	0.942 9(5)
Au(11)	0.290 48(4)	−0.013 57(4)	0.744 00(2)	C(631)	0.381(1)	0.061(2)	0.946 9(6)
P(1)	0.008 5(3)	−0.224 8(3)	0.647 9(1)	C(711)	0.372 5(8)	0.324 9(8)	0.868 1(3)

Table 5 (*Contd.*)

Atom	*x*	*y*	*z*	Atom	*x*	*y*	*z*
P(2)	0.192 5(3)	−0.329 3(3)	0.762 4(2)	C(712)	0.343 7(8)	0.274 6(7)	0.901 7(5)
P(3)	0.029 0(3)	−0.059 0(3)	0.802 9(2)	C(713)	0.386(1)	0.306(1)	0.947 4(4)
P(4)	0.149 6(3)	0.124 1(3)	0.640 4(2)	C(714)	0.457(1)	0.387(1)	0.959 7(4)
P(5)	0.321 7(3)	−0.123 1(3)	0.590 2(2)	C(715)	0.485 8(9)	0.437 6(8)	0.926 1(5)
P(6)	0.308 5(3)	−0.039 6(3)	0.909 9(1)	C(716)	0.444(1)	0.406 5(8)	0.880 3(4)
P(7)	0.315 0(3)	0.278 7(3)	0.808 3(2)	C(721)	0.214 5(7)	0.287 7(9)	0.806 3(5)
P(8)	0.495 2(3)	0.209 9(3)	0.669 8(2)	C(722)	0.213 1(8)	0.358 9(9)	0.833 4(5)
P(9)	0.515 4(3)	−0.116 1(3)	0.755 2(2)	C(723)	0.139(1)	0.370 0(9)	0.829 1(6)
P(10)	0.566 2(3)	0.189 1(3)	0.855 3(1)	C(724)	0.066 0(8)	0.310(1)	0.797 9(6)
C(111)	0.003 3(8)	−0.286 3(7)	0.592 7(3)	C(725)	0.067 4(8)	0.238 8(9)	0.770 9(5)
C(112)	0.023 6(8)	−0.241 3(6)	0.556 2(4)	C(726)	0.141 7(9)	0.227 7(8)	0.775 1(5)
C(113)	0.017 4(9)	−0.287 4(8)	0.513 5(3)	C(731)	0.370(1)	0.357(1)	0.773 0(8)
C(114)	−0.008 9(9)	−0.378 5(8)	0.507 4(3)	C(811)	0.532 4(8)	0.328 3(6)	0.691 0(4)
C(115)	−0.029 2(9)	−0.423 5(6)	0.543 9(4)	C(812)	0.557 5(9)	0.355 3(8)	0.738 5(4)
C(116)	−0.023 1(8)	−0.377 4(7)	0.586 6(4)	C(813)	0.587(1)	0.444 0(9)	0.757 5(4)
C(121)	−0.063 2(6)	−0.306 4(7)	0.675 9(4)	C(814)	0.590 8(9)	0.505 7(6)	0.729 0(5)
C(122)	−0.034 9(5)	−0.315 9(7)	0.720 3(4)	C(815)	0.566(1)	0.478 7(7)	0.681 5(5)
C(123)	−0.091 1(8)	−0.376 0(8)	0.742 5(3)	C(816)	0.536 5(9)	0.390 0(8)	0.662 5(3)
C(124)	−0.175 4(7)	−0.426 7(8)	0.720 3(4)	C(821)	0.462 5(7)	0.197 7(9)	0.607 8(3)
C(125)	−0.203 7(5)	−0.417 2(8)	0.676 0(4)	C(822)	0.376 5(7)	0.152 6(8)	0.587 5(4)
C(126)	−0.147 6(7)	−0.357 1(8)	0.653 8(3)	C(823)	0.350 2(7)	0.143 1(9)	0.540 2(4)
C(131)	−0.049(1)	−0.162(1)	0.630 5(7)	C(824)	0.409 9(9)	0.179(1)	0.513 2(3)
C(211)	0.114 4(7)	−0.371 9(8)	0.798 0(4)	C(825)	0.495 8(8)	0.224(1)	0.533 5(4)
C(212)	0.067 2(9)	−0.463 0(7)	0.793 7(5)	C(826)	0.522 1(6)	0.233 2(9)	0.580 8(4)
C(213)	0.009 0(8)	−0.496 7(6)	0.821 6(5)	C(831)	0.593(1)	0.195(1)	0.677 6(7)
C(214)	−0.002 1(8)	−0.439 4(9)	0.853 9(5)	C(911)	0.623 3(6)	−0.032 7(7)	0.760 5(5)
C(215)	0.045 0(9)	−0.348 3(8)	0.858 2(4)	C(912)	0.642 3(7)	0.014 8(9)	0.724 7(4)
C(216)	0.103 3(8)	−0.314 6(6)	0.830 3(5)	C(913)	0.724 7(8)	0.078 3(9)	0.727 1(5)
C(221)	0.271 3(7)	−0.369 4(9)	0.781 5(5)	C(914)	0.788 1(6)	0.094 4(8)	0.765 2(6)
C(222)	0.321 1(9)	−0.381 2(9)	0.751 9(4)	C(915)	0.769 1(7)	0.047(1)	0.801 0(5)
C(223)	0.386 9(8)	−0.402 7(9)	0.768 0(6)	C(916)	0.686 7(8)	−0.016 6(9)	0.798 6(4)
C(224)	0.402 9(8)	−0.412 5(9)	0.813 7(6)	C(921)	0.502 8(7)	−0.204 0(7)	0.710 4(4)
C(225)	0.353(1)	−0.400 8(9)	0.843 4(5)	C(922)	0.424 1(6)	−0.250 5(8)	0.680 6(4)
C(226)	0.287 2(9)	−0.379 2(9)	0.827 2(5)	C(923)	0.411 2(6)	−0.320 6(8)	0.647 0(4)
C(231)	0.140(1)	−0.393(1)	0.703 8(7)	C(924)	0.476 9(8)	−0.344 1(7)	0.643 2(4)
C(311)	−0.066 7(6)	−0.085 9(8)	0.759 4(4)	C(925)	0.555 6(7)	−0.297 6(8)	0.673 0(5)
C(312)	−0.068 8(7)	−0.018 7(6)	0.736 3(4)	C(926)	0.568 5(6)	−0.227 5(8)	0.706 6(4)
C(313)	−0.138 5(8)	−0.035 6(8)	0.701 8(4)	C(931)	0.516(1)	−0.166(1)	0.807 0(7)
C(314)	−0.206 0(7)	−0.120(1)	0.690 4(4)	C(1011)	0.650 3(7)	0.271 8(7)	0.833 3(4)
C(315)	−0.203 8(6)	−0.187 0(7)	0.713 4(5)	C(1012)	0.684 4(8)	0.238 7(6)	0.801 3(5)
C(316)	−0.134 2(8)	−0.170 1(7)	0.747 9(4)	C(1013)	0.750 1(8)	0.296 6(9)	0.783 2(4)
C(321)	0.030 8(9)	0.024 7(8)	0.846 6(4)	C(1014)	0.781 7(7)	0.387 6(8)	0.797 1(5)
C(322)	−0.041 4(7)	0.011 0(8)	0.864 2(5)	C(1015)	0.747 6(9)	0.420 6(6)	0.829 2(5)
C(323)	−0.039 3(8)	0.074 6(9)	0.898 4(5)	C(1016)	0.681 9(8)	0.362 8(8)	0.847 2(4)
C(324)	0.035 1(9)	0.152 0(8)	0.914 9(5)	C(1021)	0.622 4(7)	0.133 1(8)	0.885 7(4)
C(325)	0.107 3(8)	0.165 7(8)	0.897 3(5)	C(1022)	0.708 7(7)	0.178 9(7)	0.905 2(4)
C(326)	0.105 2(7)	0.102 1(9)	0.863 1(5)	C(1023)	0.750 6(6)	0.136 7(9)	0.928 9(4)
C(331)	0.007(1)	−0.153(1)	0.831 3(6)	C(1024)	0.706 1(8)	0.048 6(8)	0.933 2(4)
C(411)	0.135 7(9)	0.093 1(8)	0.578 6(3)	C(1025)	0.619 8(8)	0.002 8(6)	0.913 8(4)
C(412)	0.131 2(9)	0.011 5(7)	0.561 0(4)	C(1026)	0.578 0(6)	0.045 1(8)	0.890 1(4)
C(413)	0.116 0(9)	−0.015 1(7)	0.513 6(4)	C(1031)	0.546(1)	0.253(1)	0.900 7(6)
C(414)	0.105 3(9)	0.039 9(9)	0.483 9(3)	B(100)	0.056(2)	0.718(2)	0.388 7(9)
C(415)	0.109 8(9)	0.121 6(8)	0.501 5(4)	B(101)	0.028(2)	0.654(2)	0.334 9(9)
C(416)	0.125 1(9)	0.148 2(7)	0.548 9(4)	B(102)	0.046(2)	0.613(2)	0.383(1)
C(421)	0.203 8(8)	0.244 9(6)	0.650 6(6)	B(103)	0.137(2)	0.694(2)	0.422(1)
C(422)	0.286 3(8)	0.285 7(8)	0.643 2(6)	B(104)	0.164(2)	0.794(2)	0.403(1)
C(423)	0.326 8(7)	0.377 3(8)	0.646 8(6)	B(105)	0.102(2)	0.769(2)	0.345 2(9)
C(424)	0.284 9(9)	0.428 1(6)	0.657 8(6)	B(106)	0.088(2)	0.594(2)	0.338(1)
C(425)	0.202 5(9)	0.387 3(8)	0.665 2(7)	B(107)	0.149(2)	0.619(2)	0.388 5(9)
C(426)	0.162 0(7)	0.295 8(8)	0.661 6(6)	B(108)	0.220(2)	0.727(2)	0.398(1)
C(431)	0.042(1)	0.097(1)	0.646 6(6)	B(109)	0.204(3)	0.781(3)	0.358(1)
C(511)	0.281 6(8)	−0.242 2(6)	0.575 4(4)	B(110)	0.125(2)	0.692(2)	0.313 8(9)
C(512)	0.304 7(8)	−0.279 4(8)	0.539 2(4)	B(111)	0.188(2)	0.664(2)	0.347 6(9)
C(513)	0.268 1(9)	−0.370 9(8)	0.525 7(4)	B(200)	0.181(3)	0.259(3)	0.099(2)
C(514)	0.208 3(9)	−0.425 2(6)	0.548 4(5)	B(201)	0.244(3)	0.338(3)	0.089(2)
C(515)	0.185 1(8)	−0.388 0(7)	0.584 5(5)	B(202)	0.250(3)	0.318(3)	0.144(2)
C(516)	0.221 8(8)	−0.296 5(8)	0.598 0(4)	B(203)	0.254(3)	0.224(4)	0.145(2)
C(521)	0.435 1(8)	−0.079(1)	0.585 5(6)	B(204)	0.196(3)	0.178(3)	0.084(2)
C(522)	0.471(1)	−0.002(1)	0.566 6(7)	B(205)	0.216(3)	0.255(3)	0.051(1)
C(523)	0.556(1)	0.034(1)	0.564 9(7)	B(206)	0.338(3)	0.378(3)	0.121(2)
C(524)	0.606 7(8)	−0.006(1)	0.582 1(7)	B(207)	0.347(3)	0.309(3)	0.146(2)
C(525)	0.571(1)	−0.082(1)	0.600 9(7)	B(208)	0.316(3)	0.208(3)	0.113(2)
C(526)	0.485(1)	−0.119(1)	0.602 6(6)	B(209)	0.286(3)	0.212(3)	0.059(2)
C(531)	0.266(1)	−0.101(1)	0.539 6(6)	B(210)	0.309(3)	0.335(3)	0.062(2)
C(611)	0.353 3(9)	−0.116 2(9)	0.925 8(4)	B(211)	0.372(3)	0.308(3)	0.092(2)
C(612)	0.386(1)	−0.153(1)	0.894 3(3)				

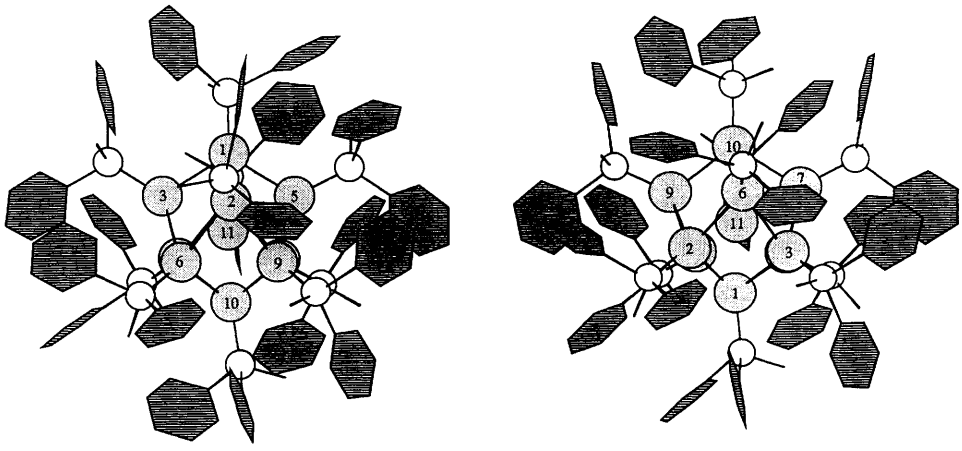

Fig. 3 Ligand packing around the metal cages in clusters (*a*) **1**·4thf and (*b*) **1**. Bonds to the central atom are omitted for clarity. The visible metal framework is labelled with serial numbers for the gold atoms

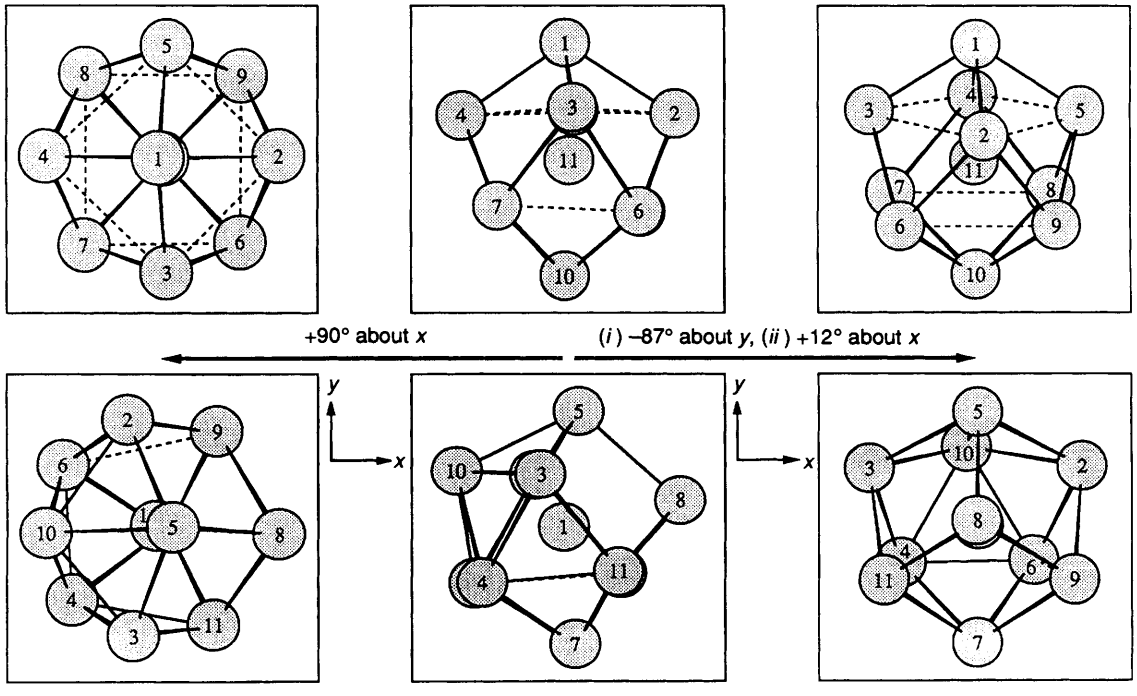

Fig. 4 The Au_{11} metal cages in clusters **1**·4thf and **2**. The three views on the top row are of the $[Au_{11}(PMePh_2)_{10}]^{3+}$ cation of **1**·4thf. Comparable views for the $[Au_{11}Cl_2(PPh_3)_8]^+$ cation of **2** are given on the bottom row. Bonds to the central atom are omitted for clarity. Metal–metal distances of less than 3.2 Å are illustrated as solid lines, whilst dashed lines are used to portray distances of between 3.2 and 3.6 Å. Positive rotations are clockwise looking along the direction of an axis

major peripheral atom movements required to convert the new undecagold geometry into the one previously reported were presented above. Such a rearrangement could transform any one of the eight crown positions into the apical atom of a three-fold cage. In reverse, three pairs of atoms opposite one another in the chair could become the apical positions of the *CBSAPR*. Interconversions of this type provide a possible mechanism to explain the fluxional behaviour of the Au_{11} cluster compounds indicated by the ^{31}P-$\{^1H\}$ NMR spectra.

In summary, the synthetic and structural studies reported in this paper have confirmed that the metal skeleton in $[Au_{11}(PMePh_2)_{10}][C_2B_9H_{12}]_3$ is based on a bicapped centred square-antiprismatic geometry, which is quite different from the C_{3v} geometry previously reported for homonuclear gold cluster compounds containing 11 metal atoms. A detailed analysis of the structure of the compound and a comparison with literature structural data has identified that the distortions in the skeleton are consistent with a reaction coordinate which converts the bicapped square antiprism into the related deltahedron with C_{3v} symmetry. These results emphasize the soft nature of the potential-energy surfaces associated with the interconversion of alternative polyhedral geometries for gold cluster compounds. Even small variations in the ligand have resulted in the change of the skeletal geometries in these Au_{11} cluster compounds. Presumably the presence of anionic ligands co-ordinated to the gold cluster leads to a structural preference for the cluster geometry with C_{3v} symmetry. These observations are also consistent with the solution NMR studies on these compounds and the observation of skeletal isomers in related gold cluster compounds.

Experimental

Elemental analyses were performed by Mr. M. Gascoigne and his staff in the Microanalytical Department of the Inorganic Chemistry Laboratory, Oxford. Electronic spectra were recorded on a UVIKON 930 spectrophotometer using a matched pair of 1 cm quartz cells. Absorption coefficients are reported as log ε_{max}, where the units of ε are $dm^3\ mol^{-1}\ cm^{-1}$. Solution NMR spectroscopy was carried out on a Bruker AM-300 spectrometer, with proton decoupling for the ^{11}B and ^{31}P

Table 6 Selected interatomic distances (Å) for the cation of cluster **1** (see Table 2 for category definitions)

Peripheral cage		Radial cage	
Category A		Category D	
Au(1)–Au(2)	2.907(1)	Au(2)–Au(11)	2.688(1)
Au(1)–Au(3)	2.905(1)	Au(3)–Au(11)	2.701(1)
Au(1)–Au(4)	2.948(1)	Au(4)–Au(11)	2.708(1)
Au(1)–Au(5)	2.910(1)	Au(5)–Au(11)	2.684(1)
Au(6)–Au(10)	2.944(1)	Au(6)–Au(11)	2.681(1)
Au(7)–Au(10)	2.910(1)	Au(7)–Au(11)	2.666(1)
Au(8)–Au(10)	2.935(1)	Au(8)–Au(11)	2.689(1)
Au(9)–Au(10)	2.883(1)	Au(9)–Au(11)	2.660(1)
Range 2.883(1)–2.98(1), mean 2.918 ± 0.022		2.660(1)–2.708(1), 2.685 ± 0.016	
Category B		Category E	
Au(2)–Au(6)	2.946(1)	Au(1)–Au(11)	2.706(1)
Au(2)–Au(9)	2.943(1)	Au(10)–Au(11)	2.760(1)
Au(3)–Au(7)	2.922(1)	2.706(1)–2.760(1), 2.733 ± 0.038	
Au(4)–Au(7)	2.960(1)		
Au(4)–Au(8)	2.952(1)		
Au(5)–Au(8)	2.945(1)		
Au(5)–Au(9)	2.945(1)		
Range 2.911(1)–2.960(1), mean 2.940 ± 0.016			
Category C		Au(*x*)–P(*x*)	
Au(2)–Au(3)	3.643(1)	Au(1)–P(1)	2.285(4)
Au(2)–Au(5)	3.678(1)	Au(2)–P(2)	2.300(4)
Au(3)–Au(4)	3.223(1)	Au(3)–P(3)	2.289(4)
Au(4)–Au(5)	3.287(1)	Au(4)–P(4)	2.294(4)
Au(6)–Au(7)	3.329(1)	Au(5)–P(5)	2.287(4)
Au(6)–Au(9)	3.732(1)	Au(6)–P(6)	2.300(4)
Au(7)–Au(8)	3.165(1)	Au(7)–P(7)	2.269(4)
Au(8)–Au(1)	3.447(1)	Au(8)–P(8)	2.296(4)
Range 3.165(1)–3.732(1), mean 3.438 ± 0.221		Au(9)–P(9)	2.277(4)
		Au(10)–P(10)	2.308(4)
		2.269(4)–2.308(4), 2.291 ± 0.012	

nuclei. For the latter, spectra were referenced to $PO(OMe)_3$–D_2O, which has a chemical shift of −2.4 ppm relative to 85% H_3PO_4. The positive-ion FAB mass spectrum was recorded using a VG AutoSpec instrument by Dr. J. A. Ballentine and his staff at the SERC Mass Spectrometry Service Centre (University College of Swansea). The sample was dissolved in CH_2Cl_2 and suspended in a matrix of 3-nitrobenzyl alcohol. The compound $PMePh_2$ was used as supplied. Samples of $[AuCl(Me_2S)]$, $[Ti(\eta\text{-}C_6H_5Me)_2]$ and $[NHMe_3][C_2B_9H_{12}]$ were prepared using literature procedures.[19–21]

Preparations

$[AuCl(PMePh_2)]$. The procedure described was carried out under N_2 using Schlenk-line techniques in a well ventilated fume cupboard. Solvents were dried and saturated with N_2. The method used was adapted from that previously reported for the preparation of $[AuCl(PBu^t_3)]$.[22] Protected from light and with vigorous stirring, $[AuCl(Me_2S)]$ (7.14 g, 24.24 mmol) was dissolved in CH_2Cl_2 (20 cm^3). To this was slowly added a solution of $PMePh_2$ (4.96 g, 24.77 mmol) in CH_2Cl_2 (20 cm^3). **CAUTION**: Me_2S is generated. The solvent was removed by passing a stream of N_2 over the reaction mixture. An oily crude product was recrystallized from CH_2Cl_2–EtOH to give a white microcrystalline sample of $[AuCl(PMePh_2)]$ (8.64 g, 19.97 mmol, 82%) (Found: C, 35.9; H, 2.8; Cl, 8.5. Calc. for $C_{13}H_{13}AuClP$: C, 36.1; H, 3.0; Cl, 8.2%); δ_P[121.50 MHz, solvent CD_2Cl_2, standard $PO(OMe)_3$–D_2O] 14.21 (1 P, s).

Cluster 1. The synthesis described is an adaptation of that reported[8] for $[Au_{11}(PMePh_2)_{10}][BPh_4]_3$ and was carried out under argon using Schlenk-line techniques. The use of dinitrogen as an inert atmosphere should be avoided. The compounds $[AuCl(PMePh_2)]$ (0.48 g, 1.11 mmol) and $[Ti(\eta\text{-}C_6H_5Me)_2]$ (0.09 g, 0.39 mmol) were cooled to 200 K in an EtOH–N_2 (l) slush bath. Previously dried and similarly cooled argon-saturated toluene (20 cm^3) was added with stirring and the temperature of the system was allowed to rise. At approximately 260 K a brown precipitate formed. After washing the solid several times with toluene to remove any excess of $[Ti(\eta\text{-}C_6H_5Me)_2]$, the brown intermediate was dissolved in EtOH (10 cm^3) and filtered. The resulting deep red solution was treated with $[NHMe_3][C_2B_9H_{12}]$ (0.10 g, 0.52 mmol) dissolved in EtOH (10 cm^3). This metathesis reaction led to immediate precipitation of a red solid which was isolated and extracted from the organic layer of CH_2Cl_2–water (1 : 1, 20 cm^3). The resulting CH_2Cl_2 solution was taken to dryness under reduced pressure. Recrystallization from thf–EtOH gave microcrystalline cluster **1** (0.26 g, 0.057 mmol, 56%) (Found: C, 35.7; H, 3.8. $C_{136}H_{166}Au_{11}B_{27}P_{10}$ requires C, 35.8; H, 3.7%); λ_{max}/nm(CH_2Cl_2) 302 (log ε 5.05), 378 (4.36) and 425 (4.58); δ_H(300.14 MHz, solvent CD_2Cl_2, standard $SiMe_4$) 7.45–6.90 (100 H, m) and 1.43 (30 H, br s); δ_B(95.25 MHz, solvent CD_2Cl_2, standard BF_3·OEt_2) −11.43 (2 B, s), −17.35 (3 B, s), −22.52 (2 B, s), −33.58 (1 B, s) and −38.27 (1 B, s); δ_P[121.50 MHz, solvent CD_2Cl_2, standard $PO(OMe)_3$–D_2O] 41.59 (10 P, s); *m*/*z* 4435 {37%, $[M + 2X]^+$, where M = $Au_{11}(PMePh_2)_{10}$ and X = $C_2B_9H_{12}$}, 3901 (100, $[M + X - 2PMePh_2]^+$), 3767 (43, $[M - 2PMePh_2]^+$), 3700 (49, $[M + X - 3PMePh_2]^+$), 3505 (76, $[M + X - Au - 3PMePh_2]^+$), 3299 (73, $[M + X - 5PMePh_2]^+$), 2968 (71, $[M - 6PMePh_2]^+$) and 2771 (71, $[M - Au - 6PMePh_2]^+$).

Crystallization experiments

Efforts to grow single crystals centred on the slow diffusion of EtOH into thf solutions of the cluster compound **1**. This was carried out in sealed, 8 mm diameter, glass tubes. Initial attempts yielded a large number of crystals that were too small for routine diffraction studies. The exercise was repeated using glass tubes previously treated with $SiCl_2Me_2$.[23] After 2 weeks there was no sign of crystal growth in any of the tubes. Over the next 3 d however, a crystal of **1**·4thf grew rapidly. Its largest dimension was over 2 mm. Cleaving several times gave an appropriate fragment that was mounted in a 0.5 mm Lindemann capillary under an atmosphere of thf-saturated dinitrogen. In one of the other glass tubes approximately 30 crystals of **1** grew over a period of months. Inspection revealed the morphology of these to be different to that already seen for **1**·4thf. A suitable crystal was mounted in a 0.3 mm Lindemann capillary, again under dinitrogen saturated with thf vapour.

Single-crystal structure determinations of clusters 1·4thf and 1

Intensity data were measured at 293 K on an Enraf-Nonius CAD4 diffractometer using graphite-monochromated molybdenum radiation (Mo-Kα, λ = 0.710 69 Å). A DEC Micro VAX 3300 computer was used to control the diffractometer and to carry out the subsequent steps involved with structure analysis. Crystallographic manipulations were carried out using the CRYSTALS suite of programs.[24] Crystal data and information relating to the data collections and structural refinements are given in Table 8. In both cases the structures were solved using direct methods[26] to give the metal atom positions. The models were subsequently developed using Fourier-difference syntheses. In both cases the cation was found to be fully ordered but the phenyl groups were idealized and refined as rigid bodies in order to reduce the number of parameters in the least-squares refinements. The hydrogen atoms of the phenyl rings were generated in calculated positions (C–H 0.96 Å), with isotropic displacement parameters 1.2 times those of the associated carbon atom.

Table 7 Summary of selected interatomic angles (°) for the cation of cluster **1** (see Table 3 for category definitions)

Cage angle category		
1	**2**	**3**
Range 65.58(2)–79.66(2)	111.29(3)–114.10(3)	55.96(2)–57.41(2)
Mean 72.30 ± 5.61	112.57 ± 1.25	56.62 ± 0.57
4	**5**	**6**
Range 98.50(3)–106.67(3)	56.98(2)–59.15(2)	82.98(2)–96.68(2)
Mean 102.58 ± 2.79	58.23 ± 0.88	90.00 ± 5.21
7	**8**	**9**
Range 64.73(2)–78.66(2)	55.91(2)–57.59(2)	64.24(2)–65.98(2)
Mean 71.63 ± 5.38	56.79 ± 0.48	65.15 ± 0.51
10	**11**	**12**
Range 109.93(3)–118.97(3)	175.14(3)	72.45(2)–88.66(3)
Mean 115.10 ± 3.51		79.77 ± 6.29
13	**14**	**15**
Range 128.49(3)–131.17(3)	65.49(2)–66.88(3)	130.41(3)–149.46(3)
Mean 129.37 ± 1.26	66.41 ± 0.48	139.37 ± 7.27
Au(11)–Au(x)–P(x)		
Range 170.0(1)–176.3(1), mean 174.04 ± 2.03		

Table 8 Details of the X-ray crystal analyses of clusters **1**·4thf and **1**[a]

	1·4thf	**1**
Chemical formula	$C_{152}H_{198}Au_{11}B_{27}O_4P_{10}$[b]	$C_{136}H_{166}Au_{11}B_{27}P_{10}$
M	4857.5[b]	4569.0
Crystal system	Monoclinic	Triclinic
Space group	$P2_1/c$ (no. 14)	$P\bar{1}$ (no. 2)
a/Å	24.747(4)	17.664(2)
b/Å	27.887(9)	16.846(1)
c/Å	25.021(6)	29.792(3)
α/°		95.469(6)
β/°	91.54(2)	98.463(8)
γ/°		114.535(6)
U/Å^3	17 260.8	7855.4
Z	4	2
D_c/Mg m^{-3}	1.87[b]	1.93
F(000)	9184[b]	4272
μ/cm^{-1}	94.3[b]	103.6
Crystal colour and shape	Red prism	Red tablet
Crystal dimensions/mm	0.68 × 0.48 × 0.31	0.33 × 0.22 × 0.08
Scan technique	ω	ω–2θ
Scan width/°	0.8 + 0.35 tan θ	0.7 + 0.35 tan θ
Scan rate/° min^{-1}	0.8–6.7	0.6–5.0
2θ Range/°	3–44	2–44
hkl Ranges	−1 to 26, −1 to 29, −26 to 26	0–18, −17 to 16, −31 to 30
Data: total, unique, observed with $I \geqslant 3\sigma(I)$	22 356, 21 038, 8567	19 931, 19 154, 10 358
Decay (%)	19	9
Transmission	0.060–0.143	0.217–0.562
R_{int}[c]	0.0411	0.0370
Observations, parameters (ratio)	9887, 1176 (8.4)	11 680, 1215 (9.6)
Chebyshev weighting scheme coefficients	16.2, −12.4, 10.4	4.60, −4.04, 3.51, −0.84
Final R, wR and restrained S[c]	0.0404, 0.0438, 1.10	0.0389, 0.0430, 1.05

[a] Details in common: empirical absorption correction (ψ scans); two-block least-squares refinement on F. [b] Based on a total solvent occupancy of 4thf in the asymmetric unit. [c] Defined in ref. 25.

In cluster **1**·4thf both the cation and anions were well ordered. The thf molecules were spread over five sites. Each solvent atom was assigned an isotropic displacement parameter of 0.25 Å^2 before the occupancies of the individual molecules were refined. In the final cycle of least-squares refinement 1176 parameters were refined in two blocks. The first contained the positional parameters, with the phenyl groups, anions and thf molecules being treated as rigid bodies. The second block consisted of the scale factor, anisotropic displacement parameters for the atoms of the cation, a joint isotropic displacement parameter for the atoms of each anion and an occupancy term for every thf molecule. Firm vibrational and slack similarity restraints[24,27] were applied to the displacement parameters within the phenyl rings.

In cluster **1** the anions were heavily disordered. In two cases the cage electron density was spread over the twelve sites of an icosahedron. This was modelled by placing twelve boron atoms on the vertices of the icosahedron and refining the occupancies, whilst restraining the sum of these to be eleven. A single isotropic displacement parameter was refined for each anion. The atomic sites of the third anion could not be resolved, even though a Fourier-difference synthesis showed the approximate position of the anion in the asymmetric unit. For the disordered anions that were located the hydrogen-atom positions were calculated (B–H 1.09). Each hydrogen was given the same occupancy as the boron atom to which it was bonded and an isotropic displacement parameter 1.2 times greater. Leading to a satisfactory agreement analysis, an isotropic extinction correction and a four-term Chebyshev weighting scheme were applied. In the final cycle of least-squares refinement 1215 parameters were refined in two blocks. The first contained positional parameters. The scale factor and anisotropic displacement parameters for the cation were refined as part of the second block. This also included the occupancy terms for

the boron atoms and the communal isotropic displacement parameter for each anion. Slack similarity and firm vibrational restraints[24,27] were applied to the displacement parameters within the phenyl rings.

Complete atomic coordinates, thermal parameters and bond lengths and angles have been deposited at the Cambridge Crystallographic Data Centre. See Instructions for Authors, *J. Chem. Soc., Dalton Trans.*, 1996, Issue 1.

Acknowledgements

The authors are grateful to the SERC for their financial support (to R. C. B. C.), Johnson Matthey plc for the loan of gold and BP plc for a generous endowment to Imperial College. Dr. F. G. N. Cloke (University of Sussex) and Dr. P. Scott (Inorganic Chemistry Laboratory, Oxford) are thanked for providing samples of $[Ti(\eta\text{-}C_6H_5Me)_2]$.

References

1 M. McPartlin, R. Mason and L. Malatesta, *Chem. Commun.*, 1969, 334.
2 P. Bellon, M. Manessero and M. Sansoni, *J. Chem. Soc., Dalton Trans.*, 1972, 1481.
3 J. M. M. Smits, P. T. Beurskens, J. W. A. van der Velden and J. J. Bour, *J. Crystallogr. Spectros. Res.*, 1983, **13**, 373.
4 J. M. M. Smits, J. J. Bour, F. A. Vollenbroek and P. T. Beurskens, *J. Crystallogr., Spectros. Res.*, 1983, **13**, 355.
5 W. Bos, R. P. F. Kanters, C. J. van Halen, W. P. Bosman, H. Behm, J. M. M. Smits, P. T. Beurskens, J. J. Bour and L. H. Pignolet, *J. Organomet. Chem.*, 1986, **307**, 385.
6 J. C. Machell, D.Phil. Thesis, University of Oxford, 1990.
7 B. R. C. Theobald, D.Phil. Thesis, University of Oxford, 1981.
8 K. P. Hall, Part II Thesis, University of Oxford, 1981.
9 C. E. Briant, B. R. C. Theobald, J. W. White, L. K. Bell and D. M. P. Mingos, *J. Chem. Soc., Chem. Commun.*, 1981, 201.
10 R. C. B. Copley and D. M. P. Mingos, *J. Chem. Soc., Dalton Trans.*, following paper.
11 F. A. Vollenbroek, J. P. van der Berg, J. W. A. van der Velden and J. J. Bour, *Inorg. Chem.*, 1980, **19**, 2685.
12 C. E. Briant, K. P. Hall and D. M. P. Mingos, *J. Chem. Soc., Chem. Commun.*, 1984, 290.
13 J. Buchanan, E. J. M. Hamilton, D. Reed and A. J. Welch, *J. Chem. Soc., Dalton Trans.*, 1990, 677.
14 R. D. Dobrott and W. N. Lipscomb, *J. Chem. Phys.*, 1962, **37**, 1779.
15 K. P. Hall, B. R. C. Theobald, D. I. Gilmore, D. M. P. Mingos and A. J. Welch, *J. Chem. Soc., Chem. Commun.*, 1982, 528.
16 J. J. Bour, W. V. D. Berg, P. P. J. Schlebos, R. F. P. Kanters, M. F. J. Schoondergang, W. P. Bosman, J. M. M. Smits, P. T. Beurskens, J. J. Steggerda and P. van der Sluis, *Inorg. Chem.*, 1990, **29**, 2971.
17 W. N. Lipscomb, *Science*, 1966, **153**, 373.
18 D. M. P. Mingos and D. J. Wales, in *Electron Deficient Boron and Carbon Clusters*, eds. G. A. Olah and K. Wade, Wiley, New York, 1991.
19 F. Bonati and G. Minghetti, *Gazz. Chim. Ital.*, 1973, **103**, 373.
20 M. T. Anthony, M. L. H. Green and D. Young, *J. Chem. Soc., Dalton Trans.*, 1975, 1419.
21 R. A. Wiesboeck and M. F. Hawthorne, *J. Am. Chem. Soc.*, 1964, **86**, 1642.
22 G. Banditelli, A. N. Bandini, F. Bonati, R. G. Goel and G. Minghetti, *Gazz. Chim. Ital.*, 1982, **112**, 539.
23 *Crystallization of Nucleic Acids and Proteins*, eds. A. Ducruix and R. Giege, IRL Press, Oxford, 1992, p. 83.
24 D. J. Watkin, J. R. Carruthers and P. W. Betteridge, *CRYSTALS User Manual*, Chemical Crystallography Laboratory, University of Oxford, 1985.
25 S. R. Hall, F. H. Allen and I. D. Brown, *Acta Crystallogr., Sect. A*, 1991, **47**, 655.
26 G. M. Sheldrick, SHELXS 86, Program for the Solution of Crystal Structures, University of Göttingen, 1986.
27 J. R. Rollett, in *Crystallographic Computing*, ed. F. R. Ahmed, Munksgaard, Copenhagen, 1970, p. 171.

Received 27*th June* 1995; *Paper* 5/04140F